

# THE INTERNATIONAL JOURNAL OF SCIENCE & TECHNOLEDGE

## Gravity Variations across Nakaporon Fault in Korosi Geothermal Prospect Field

**Namaswa Solomon Wangila**

Multimedia University of Kenya Department of Physics, Mbagathi, Nairobi, Kenya

**Ambusso Willis Jakanyango**

Kenyatta University, Department of Physics, Nairobi, Kenya

**Migwi Charles Maina**

Kenyatta University, Department of Physics, Nairobi, Kenya

### **Abstract:**

*Study of the alignment of faults is important since faults play a major role in mineral, petroleum, geothermal and hydrogeological distribution. In this study, gravity survey in the target region was conducted by the use of Sodin gravity meter to detect variations in density of the rocks across Nakaporon fault in Korosi geothermal prospect field. A total of 68 gravity stations were surveyed across Nakaporon fault. Data was processed to remove all other effects not related to the subsurface density changes. Using surfer software, a grid and contour map was created and then sliced to obtain three gravity profiles that were oriented across the anomaly. From the three profiles, it was established that eastern side had high gravity and displaced upward while the western side had lower gravity and displaced downward forming a normal fault that ran in the NNE direction.*

**Keywords:** gravity, fault, korosi geothermal

### **1. Introduction**

Faults have been identified as crucial in understanding geothermal systems since they influence the stratigraphic structure, and how this structure influences fluid flow. Fault networks influence not only conventional geothermal plays, but also hot sedimentary aquifers. Knowledge of the subsurface structure, and knowing the likelihood and location of faults is crucial for understanding the source and movement of heat. Korosi geothermal prospect field is located in Baringo county in the great East Africa rift valley approximately 400km north- northwest of Nairobi on the coordinates 0°46'N 36°07'E. It is bounded to the east and west by escarpments that are controlled by faults and monoclinical warps and has a marked northward gradient (Omenda, 2011). Nakaporon and Nagoreti being two of the faults that passes through the area. Korosi is one of the main volcanoes in the northern rift floor rising to about 500 m above the surrounding floor of the trough and covers an area of about 260 km<sup>2</sup>.

The Nakaporon fault runs on the western side of Korosi, faulted in the NNE direction. Korosi volcanic complex is one of several major volcanic centres in the Central Kenya Rift of the East African Rift system in the north of Lake Baringo.

In the Perth metropolitan area of Australia, identification and geothermal influence of faults was carried out by Carbel et al, 2012. Field observation was identified as the easiest way of fault identification where major deep aquifers that are highly faulted throughout the basin but fault covered by younger sediments were unable to be identified by physical observation. Seismic observation and refraction was not easy to be carried out in the densely populated residential area. Electromagnetic and magnetic methods were found to be influenced by noise sources in the densely populated urban area.

Gravity data was used to investigate the depths to discontinuities beneath the Adamawa plateau region, Central Africa and the data revealed steep north east trending gradient in the bouguer gravity anomalies that coincided with the Sanaga fault zone and the Fuamban shear zone lying between the Adamawa plateau (Nnange et al., 2000).

### **2. Data Acquisition**

The Sodin type gravimeter and a Germin hand held Global Positioning System (GPS) were used in the field survey. The Sodin type gravimeter was used to determine the vertical component of the gravitational component,  $g_z$ . The base station was first established from where gravity differences along the other stations were measured. The gravimeter was set up by first setting up the tripod using the extension legs. Using the target level at the centre of the tripod, it was leveled so that the spirit level is exactly at the middle. The gravity meter was then placed on the tripod table and leveled by the use of the concave surface of the tripod and the foot screws of the meter.

The Germin GPS was then switched on and latitude, longitude, altitude and time and were also recorded. This process was repeated in all the stations gravity was recorded. The base station was set and readings were taken at the start and end of the exercise. A total of 68 gravity stations were surveyed across Nakaporon fault as shown in the figure 1 below with a distance between gravity stations ranging between 10- 50 meters interval. These stations were located along the 3 profiles across the

Nakaporon fault. The gravity meter was leveled over the survey mark before taking, the time, date; dial reading, station number and elevation of the station with sea level as the reference point were recorded.

## 2.1. Data Processing

### 2.1.1. Drift Correction

The counter readings were first converted to milligals by multiplying the meter constant shown on the small plate on the counter top. Then the empirical drift correction using base station readings was applied. This was to correct for variations in gravimeter reading at the same station during the day as a result of changes in mechanical properties of the gravimeter. It was done by establishing a base station at which the readings were taken twice during the day, at the start and end of the daily readings and readings made in one station assumed to have a linear drift as fitted base readings. The first and the last readings were often taken at the base station for each survey day. After the data collection, the drift effect was calculated and the gravity data were filtered by using the following:

$$\text{Drift} = \frac{G_{\text{base}, f} - G_{\text{base}, i}}{T_{\text{base}, f} - T_{\text{base}, i}}$$

Where, *Drift* is the drift rate of measurement.

$G_{\text{base}, f} - G_{\text{base}, i}$  are the final and initial total gravity field measurements at the base station,  $T_{\text{base}, f} - T_{\text{base}, i}$  are the final and initial time at the base station.

The drift corrected field at any station in the loop for a given day was calculated from:

$$D_{\text{Drift}, n} = G_n * (T_n - T_i)$$

Where  $D_{\text{Drift}, n}$  is the drift corrected gravity at the *n*th station.

$G_n$  is the total gravity at the *n*th station.

$T_n$  is the measuring time at the *n*th station.

$T_i$  is the measuring time at the first station of the loop.

### 2.1.2. Latitude Correction

The mathematical formula used to predict the components of the gravitational acceleration produced by the earth's shape and rotation is called the Geodetic Reference Formula of 1967 was used to give the gravity value that would result if the Earth were a perfect spheroid. The value  $g_\phi$  is given by:

$$g_\phi = 978.03185(1 + 0.005278895 \sin^2 \phi - 0.000023462 \sin^4 \phi) \text{ m/s}^2$$

$\phi$  is measured in radians. This value was calculated using the Eastings and Northings of the particular station by using Magpick UTM (Gauss-Kruger) Transformation setup software

The value obtained from equation was subtracted from the measured value to isolate the latitude effect.

This gravity value was first calculated for each base station and then subtracted from all other values tied to that station to find the relative latitude correction.

### 2.1.3. Free Air Correction (FAC)

For each of the field stations free air correction was calculated. The value of FAC at the base station was subtracted from all other stations to give the relative FAC.

This value was added to the latitude corrected gravity to obtain the free air corrected gravity at a particular station.

### 2.1.4. Bouguer Correction (BC)

BC was computed with a density value of  $2.67 \text{ gm}^{-3}$  from the equation  $BC = 0.4191\rho h$ , where  $\rho$  is the average density of the rocks underlying the survey area. It was then subtracted from FAA to arrive at the Simple Bouguer Anomaly (SBA). For each station this effect was calculated. The value of BC calculated for the base station was then subtracted from all other stations tied to that base station to give relative BC.

After simple bouguer anomaly corrections, the base stations were taken as reference points and all the data collected during each day were treated with reference to the base stations. The gravity data were gridded using surfer software using Kringing method. Data were saved as grid files (GRD format). The grid files were then imported by surfer software using the Grid Node Editor and saved as DAT files. Profiles across the anomaly were drawn and using Microsoft Excel™, modeling was performed to create curves that resemble the profiles.

**2.1.5. The Bouguer Anomaly Map**

A contour map, constructed using a computer program surfer, shows simple gravity data as gathered in the field (Fig. 2). The Bouguer anomaly map with a contour interval of 0.5 mGal and a maximum of 6 mGal and a minimum of -5.5 mGal were drawn. There is a correlation between several mapped topography shape and gravity values. The relatively large anomaly had a shape which roughly follows NNE trend of the study area. There was a reduction in gravity at 176000 Easting as one move from west to east. The gravity drastically starts rising again as from 176400 Easting. Gravity is higher on the eastern side than the western side.

**2.1.6. Selection of profiles**

Using surfer software, a grid and contour map was created and then sliced to obtain the gravity profile. The profiles chosen were oriented across the anomaly in the direction E-W as shown in figure 2. The simple relative Bouguer anomaly contour lines were used in plotting of the profiles. From the three profiles in figures 3, 4 and 5, the gravity data revealed that eastern side had high gravity and displaced upward while the western side had lower gravity and displaced downward forming a normal fault that ran in the north to south direction.

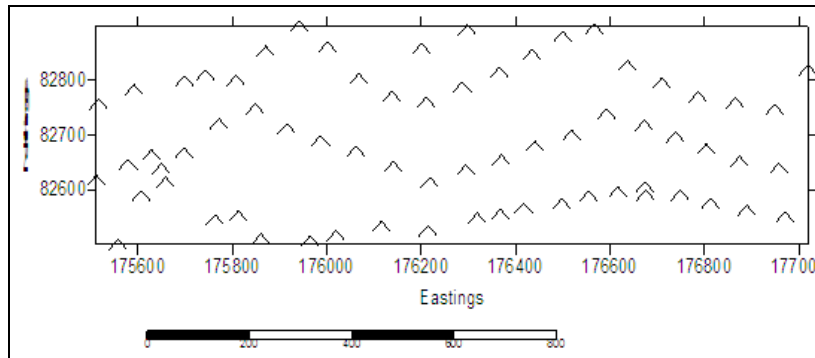


Figure 1: Station distributions for the gravity survey across Nakaporon fault

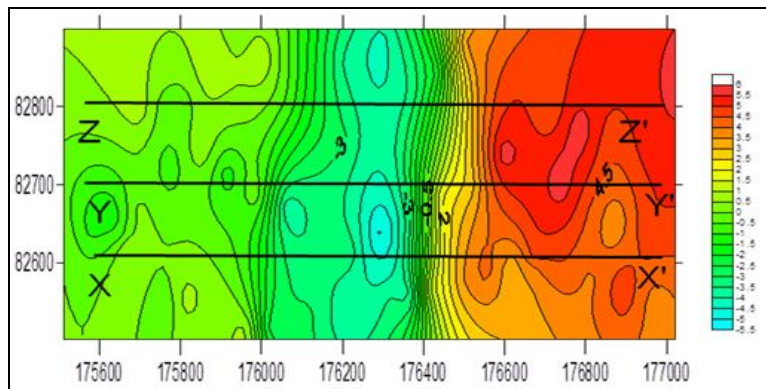


Figure 2: Bouguer gravity anomaly profiles

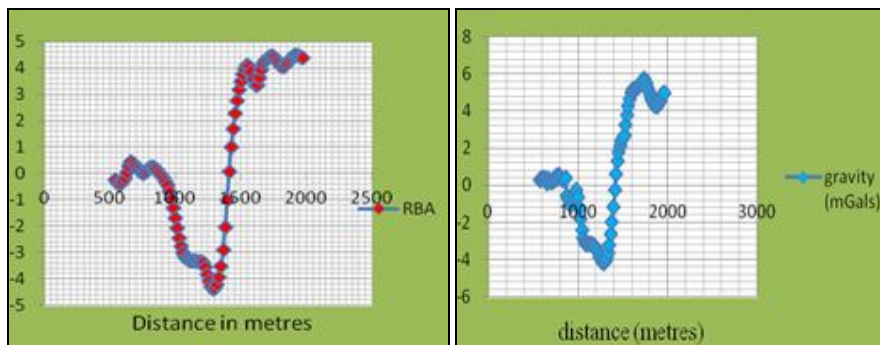


Figure 3: Observed Bouguer gravity anomaly along profile XX' and the estimated trend.

Figure 4: Observed Bouguer gravity anomaly along profile YY' and the estimated trend

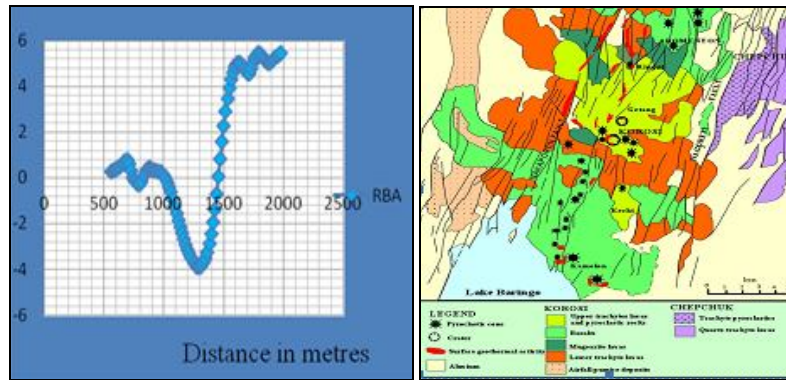


Figure 5: Observed Bouguer gravity anomaly along profile ZZ' and the estimated trend

Figure 6: Figure 2 Geological Map of Korosi

### 3. Conclusion

Gravity survey conducted revealed that eastern side had high gravity and displaced upward while the western side had lower gravity and displaced downward forming a normal fault that ran in the north to south direction.

### 4. Acknowledgement

We acknowledge Kenyatta University, Physics Department for availing the survey instruments.

### 5. References

1. Alfreda, L. (2004). Identification of fault zones using gravity Survey and subsurface exploration: A case study. University of Hong Kong.
2. Babae, M., Alvandi, A. and Zomorrodian, H. (2011). Estimation of Depth and Shape Factor of Buried Structure from Residual Gravity Anomaly Data. Australian Journal of Basic and Applied Sciences, 5(11): 2011-2015
3. Corbel, S., Schilling, O., Horowitz, F. G., Reid, L. B., Sheldon, H. A., Timms, N. E. and Wilkes, P. (2012). Identification and geothermal influence of faults In the Perth Metropolitan area, Australia. Proceedings, Thirty-Seventh Workshop on Geothermal Reservoir Engineering Stanford University, Stanford, California, January 30 - February 1, 2012.
4. Cooper, M. S., Tianyou, L. and Mbue, N. I. (2010). Fault Determination Using One Dimensional Wavelet Analysis. Journal of American Science 6:7
5. Holom, D. I. and Oldow, J. S. (2006). Gravity Reduction Spreadsheet To Calculate The Bouguer Anomaly Using Standardized Methods And Constants. Department of Geological Sciences, University of Idaho, Moscow, Idaho 83844-3022, USA
6. Murra, A. S. and Tracey, R. M. (2006). Best Practice in Gravity Surveying. Australian Geological survey Organization
7. Nnange, J. M., Ngako, V., Fairhead, J. D. and Ebinger, C. J., (2000). Depths to density discontinuities beneath the Adamawa Plateau region, Central Africa, from spectral analysis of new and existing gravity data. Journal of African Earth Sciences. 30, 887-901.
8. Ofwona, C., Omenda, P., Mariita, N., Wambugu, J., Mwawongo, G. and Kubo, B. (2006). Surface geothermal exploration of Korosi and Chepchuk prospects. KenGen internal report.
9. Omenda, P. A. (2006). THE Geology And Geothermal Activity of The East African Rift Presented at Short Course VI on Exploration for Geothermal Resources, at Lake Bogoria and Lake Naivasha, Kenya, Oct. 27 – Nov. 18, 2011.
10. Omenda, P. A. (2007). Status of geothermal exploration in Kenya and future plans for its development. Presented at Short Course II on Surface Exploration for Geothermal Resources, organized by UNU-GTP and KenGen, at Lake Naivasha, Kenya, 2-17 November, 2007.
11. Toughmalani R. (2010). Application of Gravity Method in Fault Path Detection. Australian Journal of Basic and Applied Sciences, 4: 6450-6460